



Published in final edited form as:

Org Lett. 2014 January 3; 16(1): 266–269. doi:10.1021/ol403241v.

## Callyspongiolide, a Cytotoxic Macrolide from the Marine Sponge *Callyspongia* sp

Cong-Dat Pham<sup>†</sup>, Rudolf Hartmann<sup>‡</sup>, Philip Böhler<sup>§</sup>, Björn Stork<sup>§</sup>, Sebastian Wesselborg<sup>§</sup>, Wenhan Lin<sup>⊥</sup>, Daowan Lai<sup>\*,†</sup>, and Peter Proksch<sup>\*,†</sup>

<sup>†</sup>Institute of Pharmaceutical Biology and Biotechnology, Heinrich-Heine University, 40225 Düsseldorf, Germany

<sup>§</sup>Institute of Molecular Medicine, Heinrich-Heine University, 40225 Düsseldorf, Germany

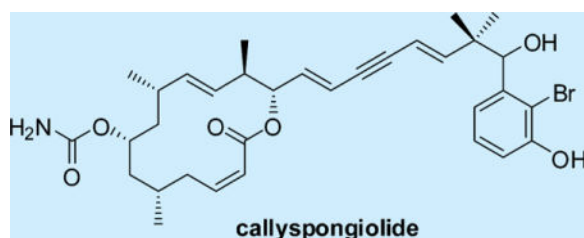
<sup>‡</sup>Institute of Complex Systems (ICS-6), Forschungszentrum Jülich GmbH, 52425 Jülich, Germany

<sup>⊥</sup>State Key Laboratory of Natural and Biomimetic Drugs, Peking University, Beijing 100191, PR China

### Abstract

A novel macrolide, callyspongiolide, whose structure was determined by comprehensive analysis of the NMR and HRMS spectra, was isolated from the marine sponge *Callyspongia* sp. collected in Indonesia. The compound features a carbamate-substituted 14-membered macrocyclic lactone ring with a conjugated structurally unprecedented diene-ynic side chain terminating at a brominated benzene ring. Callyspongiolide showed strong cytotoxicity against human Jurkat J16 T and Ramos B lymphocytes.

### Graphical abstract



Macrolides have been reported from various marine macroorganisms<sup>1</sup> but are especially prominent for marine sponges as exemplified by the discovery of dictyostatin,<sup>2</sup> lasonolide A,<sup>3</sup> peloruside A,<sup>4</sup> salicylihalamides A and B,<sup>5</sup> candidaspongiolides A and B,<sup>6</sup> and leiodermatolide.<sup>7</sup> Many macrolides display potent antiproliferative properties against cancer

<sup>\*</sup>Corresponding Authors: Daowan Lai, laidaowan123@gmail.com; Peter Proksch, proksch@uni-duesseldorf.de.

#### Supporting Information

Experimental procedures, sponge material, extraction and isolation, characterization data of **1**, cell viability assay, and copies of IR, UV, 1D and 2D NMR, and HRMS spectra of **1**. This material is available free of charge via the Internet at <http://pubs.acs.org>.

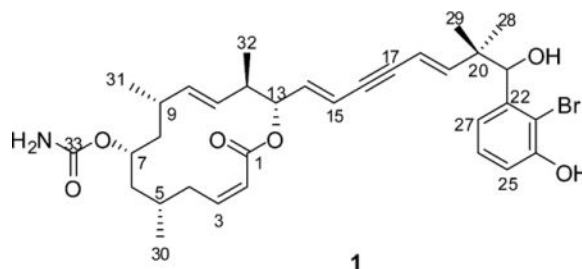
#### Notes

The authors declare no competing financial interest.

cells, making them promising leads for the development of new chemotherapeutic agents.<sup>8</sup> Due to their unusual structures and pronounced bioactivity, these compounds continue to be exciting targets for realizing a total synthesis,<sup>8c,d,9</sup> which could not only confirm or solve the stereochemistry of the structure but also contribute to further biochemical or clinical investigations that may be initially hampered by their low natural abundance.

Sponges belonging to the genus *Callyspongia* have proven to be rich sources of various cytotoxic substances, such as polyketides,<sup>10</sup> polyacetylenes,<sup>11</sup> alkaloids,<sup>12</sup> and cyclic peptides.<sup>13</sup> Macrolides, however, have not been reported from this genus prior to this study. In our search for bioactive metabolites from marine organisms,<sup>14</sup> we observed that a methanolic extract of the sponge *Callyspongia* sp., collected in Indonesia, completely inhibited the growth of the murine lymphoma cell line L5178Y at a concentration of 10  $\mu\text{g}/\text{mL}$ . Chromatographic separation of the extract afforded a new bioactive macrolide, named callyspongiolide (**1**) (4.6 mg, 0.00092% wet weight). Herein, we report the structure elucidation, configurational analysis, and cytotoxic activity of the first macrolide discovered from the genus *Callyspongia*.

Callyspongiolide (**1**) was obtained as a light yellowish amorphous solid. The ESIMS spectrum of **1** showed pseudomolecular ion peaks ( $[\text{M} + \text{Na}]^+$ ) at  $m/z$  650 and 652 with approximately the same intensity, indicating the presence of one bromine atom in **1**. Its molecular formula was established as  $\text{C}_{33}\text{H}_{42}\text{BrNO}_6$  by HRESIMS measurement, as a prominent pseudomolecular ion peak was observed at  $m/z$  650.2085  $[\text{M} + \text{Na}]^+$ . The  $^1\text{H}$  NMR spectrum showed signals attributable to three aromatic protons [ $\delta_{\text{H}} = 7.13$  (t), 6.84 (dd), 6.83 ppm (dd)], eight olefinic protons [ $\delta_{\text{H}} = 6.36$  (d), 6.13 (td), 6.06 (dd), 5.94 (dd), 5.93 (dd), 5.46 (dd), 5.22 (dd), 5.06 ppm (dd)], three oxygenated methine protons [ $\delta_{\text{H}} = 5.09$  (dd), 4.89 (d), 4.47 ppm (br.dd)], and five methyl groups [ $\delta_{\text{H}} = 1.04$  (s), 0.97 (d), 0.96 (s), 0.89 (d), 0.87 ppm (d)] (see Table S1 in Supporting Information). In the  $^{13}\text{C}$  NMR spectrum (Table S1), 33 resonances were clearly seen, which were assignable to one ester group ( $\delta_{\text{C}} = 164.2$  ppm), one carbamate group ( $\delta_{\text{C}} = 156.7$  ppm), one benzene ring ( $\delta_{\text{C}} = 153.3, 143.2, 126.9, 120.1, 114.3, 111.7$  ppm), eight olefinic carbons ( $\delta_{\text{C}} = 151.6, 142.5, 139.6, 136.4, 132.0, 122.3, 113.4, 106.8$  ppm), one alkyne group ( $\delta_{\text{C}} = 90.4, 86.3$  ppm), and 15  $\text{sp}^3$  hybrid carbons. These functionalities account for 12 of the total 13 degrees of unsaturation as required by the molecular formula, thus implying that one additional ring is present in the structure of **1**.



Detailed analysis of the phase-sensitive COSY spectrum allowed the assignment of a long continuous spin system, which started from the olefinic proton, CH-2 [ $\delta_{\text{H}} = 5.93$  ppm (dd)], and sequentially extended until the olefinic proton, CH-15 [ $\delta_{\text{H}} = 5.94$  ppm (dd)] (Figure 1).

In the  $^1\text{H}$  NMR spectrum, resonances for three pairs of olefinic protons were discernible, which were assigned to three disubstituted double bonds that were placed at C-2/3, C-10/11, and C-14/15, respectively. In addition, three methyl groups (Me-30/31/32) were enclosed in this unit, which were coupled to methine protons at C-5, C-9, and C-12, respectively, as evident by the COSY spectrum. One oxymethine proton that resonated at 4.47 ppm was located at C-7, as it showed COSY correlations to  $\text{CH}_2$ -6 and  $\text{CH}_2$ -8. This conclusion was secured by analysis of the HMBC spectrum, since correlations from Me-30 [ $\delta_{\text{H}} = 0.97$  ppm (d)] to C-4 ( $\delta_{\text{C}} = 31.3$  ppm), C-5 ( $\delta_{\text{C}} = 26.9$  ppm), and C-6 ( $\delta_{\text{C}} = 41.1$  ppm); Me-31 [ $\delta_{\text{H}} = 0.87$  ppm (d)] to C-8 ( $\delta_{\text{C}} = 44.1$  ppm), C-9 ( $\delta_{\text{C}} = 33.2$  ppm), and C-10 ( $\delta_{\text{C}} = 136.4$  ppm); Me-32 [ $\delta_{\text{H}} = 0.89$  ppm (d)] to C-11 ( $\delta_{\text{C}} = 132.0$  ppm), C-12 ( $\delta_{\text{C}} = 41.8$  ppm), and C-13 ( $\delta_{\text{C}} = 75.7$  ppm); and H-7 to C-5, C-6, C-8, and C-9 were discerned (Figure 1). The further HMBC correlation from H-7 to the carbamate group ( $\delta_{\text{C}} = 156.7$  ppm, C-33) suggested this group being located at C-7. The second oxymethine [ $\delta_{\text{H}} = 5.09$  ppm (dd);  $\delta_{\text{C}} = 75.7$  ppm] was assigned to CH-13 as indicated by analysis of the COSY and HMBC spectra (Figure 1). The key HMBC correlations from H-13 [ $\delta_{\text{H}} = 5.09$  ppm (dd)], H-2 [ $\delta_{\text{H}} = 5.93$  ppm (dd)], and H-3 [ $\delta_{\text{H}} = 6.13$  ppm (td)] to the ester carbonyl ( $\delta_{\text{C}} = 164.2$  ppm, C-1) allowed the establishment of a 14-membered macrocyclic ring in **1** with a C-14/15 double bond in the side chain.

The remaining resonances of two olefinic protons [ $\delta_{\text{H}} = 5.46$  (dd), 6.36 ppm (d)] were assigned to the fourth disubstituted double bond (C-18/19). An alkyne group was present in the side chain of **1**, which was consistent with the  $^{13}\text{C}$  NMR chemical shifts ( $\delta_{\text{C}} = 86.3, 90.4$  ppm). This group was enveloped by two disubstituted double bonds (i.e.,  $^{14}$  and  $^{18}$ ), as evident by the HMBC correlations observed from H-14 [ $\delta_{\text{H}} = 6.06$  ppm (dd)] to C-16 ( $\delta_{\text{C}} = 86.3$  ppm); H-15 [ $\delta_{\text{H}} = 5.94$  ppm (dd)] to C-17 ( $\delta_{\text{C}} = 90.4$  ppm); H-18 [ $\delta_{\text{H}} = 5.46$  ppm (dd)] to C-16, C-17; and H-19 [ $\delta_{\text{H}} = 6.36$  ppm (d)] to C-17, which thus concluded a conjugated diene-ynic moiety. Notably, in this unsaturated system with  $\text{sp}$ -hybridized carbons, typical long-range correlations were observed through 4 or 5 bonds. For example, H-15 and H-18 were coupled to each other with coupling constant of 2.2 Hz ( $^5J$ ), while HMBC correlations were found from H-18 to C-14 ( $\delta_{\text{C}} = 139.6$  ppm) and C-15 ( $\delta_{\text{C}} = 113.4$  ppm), and from H-19 to C-16 (Figure 1).

The two remaining methyl groups, Me-28 [ $\delta_{\text{H}} = 1.04$  ppm (s)] and Me-29 [ $\delta_{\text{H}} = 0.96$  ppm (s)], were deduced to be connected to a quaternary carbon (C-20,  $\delta_{\text{C}} = 43.0$  ppm), since both of them appeared as a singlet in the  $^1\text{H}$  NMR spectrum and showed HMBC correlations to C-20. A hydroxyl-bearing methine was assigned to C-21, as evident by its chemical shifts [ $\delta_{\text{H}} = 4.89$  ppm (d),  $\delta_{\text{C}} = 76.5$  ppm] and the COSY correlation between H-21 and OH-21 [ $\delta_{\text{H}} = 5.49$  ppm (d)]. The HMBC correlations from Me-28/29 to C-19 ( $\delta_{\text{C}} = 151.6$  ppm) and C-21 established the linkage between the diene-ynic group and C-21 through C-20. In addition, a 1,2,3-trisubstituted benzene ring was revealed by analysis of the coupling pattern of the aromatic protons [ $\delta_{\text{H}} = 6.83$  (dd,  $J = 7.9, 1.3$  Hz), 7.13 (t,  $J = 7.9$  Hz), and 6.84 ppm (dd,  $J = 7.9, 1.3$  Hz); an ABC spin system], in which one hydroxyl group was substituted at C-24 as supported by the HMBC correlations from OH-24 [ $\delta_{\text{H}} = 10.04$  ppm (s)] to C-23 ( $\delta_{\text{C}} = 111.7$  ppm), C-24 ( $\delta_{\text{C}} = 153.3$  ppm), and C-25 ( $\delta_{\text{C}} = 114.3$  ppm), while CH-21 was attached to C-22, as H-21 showed HMBC correlations to C-22 ( $\delta_{\text{C}} = 143.2$  ppm), C-23, and

C-27 ( $\delta_{\text{C}} = 120.1$  ppm) (Figure 1). Thus, the third substituent in the aromatic ring had to be a bromine atom to complete the whole molecule of **1**. The geometry of the double bonds was deduced to be *2Z*, *10E*, *14E* and *18E* on the basis of the proton–proton coupling constants ( $J_{2,3} = 12.0$  Hz,  $J_{10,11} = 15.0$  Hz,  $J_{14,15} = 15.8$  Hz,  $J_{18,19} = 16.4$  Hz).

Callyspongiolide thus features a carbamate-substituted 14-membered macrocyclic lactone ring with a structurally unprecedented unsaturated side chain that incorporates a conjugated diene-yne and terminates at a brominated benzene ring. Callyspongiolide contains six stereogenic centers, including five in the macrocyclic ring and one in the side chain, which are spatially segregated.

The chemical shift differences of methylene protons and the presence of both large and small  $^1\text{H}$ – $^1\text{H}$  coupling constants at centers throughout the molecule that were not dependent on the NMR solvent used (DMSO- $d_6$ , MeOH- $d_4$ ) suggested the presence of a single predominant conformer.<sup>15</sup> Thus, the relative configuration of the stereocenters in the macrocyclic ring was deduced by combined analysis of the ROESY correlations and of the homonuclear ( $^3J_{\text{H,H}}$ ) and heteronuclear ( $^{2,3}J_{\text{C,H}}$ ) coupling constants.<sup>7,16</sup>

The relative configuration of C-4 to C-9 is shown in Figure 2A. The small vicinal coupling constants of H-5/H-4a (4.8 Hz) and H-5/H-4b (3.0 Hz) suggested *gauche* relationships between these protons, while the large  $^3J_{\text{H-4a, C-30}}$  (8.6 Hz) and small  $^3J_{\text{H-4b, C-30}}$  (3.0 Hz) couplings indicated an *anti* relationship between H-4a and Me-30 and a *gauche* relationship between H-4b and Me-30. Small  $^3J_{\text{H-6a, H-5}}$  (3.0 Hz) and  $^3J_{\text{H-6a, C-30}}$  (2.3 Hz) couplings defined the *gauche* relationships of H-6a/H-5 and H-6a/Me-30. Similarly, the *gauche* relationships of Me-30/H-6b and C-7/H-5 were consistent with the small coupling constants of  $^3J_{\text{H-6b, C-30}}$  (1.5 Hz) and  $^3J_{\text{H-5, C-7}}$  (~0 Hz). A large coupling constant of 11.4 Hz between H-6a and H-7 established the antiperiplanar relationship of both protons, while the small  $^3J_{\text{H-6b, C-8}}$  (1.0 Hz) coupling served to define the *gauche* relationship between H-6b and C-8. An *anti* relationship between H-7 and H-8a was inferred from the large  $^3J_{\text{H-7, H-8a}}$  (10.1 Hz) coupling. The observation of a small coupling constant (1.0 Hz) between H-8b and C-6 established the *gauche* relationship between C-9 and the carbamate group. A large coupling (7.3 Hz) between H-8a and C-10 suggested their *anti* relationship, while a small  $^3J_{\text{H-9, C-7}}$  (3.2 Hz) coupling indicated the *gauche* relationship between H-9 and C-7, which was consistent with the  $^3J_{\text{H-8b, C-31}}$  (1.1 Hz) and  $^3J_{\text{H-8a, C-31}}$  (4.1 Hz) values. Taken together with the aforementioned conformational analysis, the relative stereochemical assignment of C-4 to C-9 was completed.

Similarly, the relative configuration of the remaining stereocenters (C-12 and C-13) within the macrocyclic ring was deduced by analysis of NOE and coupling constants. The large coupling (10.1 Hz) between H-12 and H-13 together with the ROESY correlations of Me-32/H-14 and H-12/H-14 established the relative configuration of C-12 and C-13 (Figure 2B). Moreover, the large coupling constants between H-9/H-10 (9.1 Hz), H-10/H-11 (15.0 Hz), H-11/H-12 (9.3 Hz), H-12/H-13 (10.3 Hz), H-13/H-14 (7.7 Hz), and H-14/H-15 (15.8 Hz), in association with the observed ROESY correlations between H-10, H-12, and H-14 and between H-9, H-11, H-13, and H-15 revealed the pseudoplanar nature of the C9–C13 backbone, in which vicinal protons were *anti* configured, as depicted in Figure 2B.

This preferred conformation was important for assigning the relative configuration of the stereocenters within C5–C9 and C12–C13, as the C8 chain and O–C1 had to be cofacial in the pseudoplanar C9–C13 system to close the macrocyclic ring. As such, an *S*\* configuration of C-9 would lead to the interpretation of 12*R*\* and 13*S*\* configuration. The relative configuration of stereocenters within the macrocyclic core was thus established. Further analysis of the ROESY spectrum corroborated the foregoing stereochemical assignment. Notably, transannular correlations were observed from H-7 to H-5, H-9, H-4a, and H-11; from H-8b to H-10; and from H-10 to H-12, which suggested that H-4a, H-5, H-7, H-9, and H-11 were situated to a same face of the macrocyclic ring, while H-8b, H-10, and H-12 were directed to the opposite face (Figure S1, see Supporting Information).

The configuration of the sole stereocenter (C-21) in the side chain remained to be defined. We attempted to determine the absolute configuration of C-21 by using the modified Mosher's method.<sup>17</sup> For this purpose, **1** was treated with diazomethane to methylate the phenolic group prior to react with the (*R*)- or (*S*)-MTPACl. However, the latter reactions failed to give the corresponding MTPA esters, possibly due to the steric hindrance of C21. Hence, the absolute configuration of the stereocenters within this molecule was not assigned.

Callyspongiolide (**1**) was examined for its effects on the growth of L5178Y mouse lymphoma cells *in vitro* using the MTT assay.<sup>18</sup> It showed potent cytotoxicity in a submicromolar concentration with an IC<sub>50</sub> value of 320 nM, which is approximately 13-fold more active than the positive control kahalalide F (IC 4.3 μM).<sup>18</sup> More pronounced inhibitory activities were observed when tested against human Jurkat J16 T and Ramos B lymphocytes, which exhibited IC<sub>50</sub> values of 70 and 60 nM, respectively, after 48 h of treatment (Figure S13A in Supporting Information). This compound was further examined for its capacity to induce the generation of hypodiploid nuclei in Jurkat J16 T and Ramos B lymphocytes, and the results showed that it exhibited half maximal effective concentration (EC<sub>50</sub>) at 80 and 50 nM, respectively, after 48 h of treatment (Figure S13B). Of note, the effect of callyspongiolide (**1**) on viability could not be blocked by the parallel treatment with QVD-OPh, a caspase-inhibitor (Figure S13C). This suggests that callyspongiolide (**1**) induces cell death in a caspase-independent fashion.

In summary, callyspongiolide (**1**) is a structurally unique polyketide-derived macrolide isolated from the marine sponge *Callyspongia* sp. Notably, this macrolide features a conjugated diene-ynic side chain ending at a brominated benzene ring, which is unprecedented among all marine macrolides reported so far. The potent activity of **1** makes it a potential lead for the development of anticancer drugs. Moreover, the unique structure of this compound would make it also an interesting target for realizing a total synthesis. Studies toward this aim will finally solve the stereochemical puzzles encountered in this report.

## Supplementary Material

Refer to Web version on PubMed Central for supplementary material.

## Acknowledgments

The financial support by grant of the BMBF to P.P. is gratefully acknowledged. We wish to acknowledge the help and support of Dr. Elizabeth Ferdinandus (University of Ambon, Indonesia) during sponge collection and of Dr. Nicole de Voogd (Leiden, Naturalis Biodiversity Center, Leiden, The Netherlands) for identification of the sponge. We are indebted to Prof. W. E. G. Müller (Johannes Gutenberg University, Mainz, Germany) for cytotoxicity assays against L5178Y mouse lymphoma cells. We want to thank Dr. Victor Wray (Helmholtz Centre for Infection Research, Braunschweig, Germany) for helpful discussions and Mrs. C. Kakoschke (Helmholtz Centre for Infection Research) for measuring some NMR spectra.

## References

1. Blunt JW, Copp BR, Keyzers RA, Munro MHG, Prinsep MR. *Nat Prod Rep.* 2013; 30:237. and the previous reviews in this series. [PubMed: 23263727]
2. Pettit GR, Cichacz ZA, Gao F, Boyd MR, Schmidt JM. *J Chem Soc, Chem Commun.* 1994:1111.
3. Horton PA, Koehn FE, Longley RE, McConnell OJ. *J Am Chem Soc.* 1994; 116:6015.
4. West LM, Northcote PT, Battershill CN. *J Org Chem.* 2000; 65:445. [PubMed: 10813954]
5. Erickson KL, Beutler JA, Cardellina JH II, Boyd MR. *J Org Chem.* 1997; 62:8188. [PubMed: 11671930]
6. Whitson EL, Pluchino KM, Hall MD, McMahon JB, McKee TC. *Org Lett.* 2011; 13:3518. [PubMed: 21644548]
7. Paterson I, Dalby SM, Roberts JC, Naylor GJ, Guzmán EA, Isbrucker R, Pitts TP, Linley P, Divlianska D, Reed JK, Wright AE. *Angew Chem, Int Ed.* 2011; 50:3219.
8. (a) Higa, T.; Tanaka, J. Bioactive marine macrolides. In: Atta ur, R., editor. *Studies in Natural Products Chemistry.* Vol. 19. Elsevier; Amsterdam: 1996. p. 549-626.(b) Napolitano JG, Daranas AH, Norte M, Fernandez JJ. *Anti-Cancer Agents Med Chem.* 2009; 9:122.(c) Yeung K-S, Paterson I. *Chem Rev.* 2005; 105:4237. [PubMed: 16351045] (d) Lorente A, Lamariano-Marketegi J, Albericio F, Álvarez M. *Chem Rev.* 2013; 113:4567. [PubMed: 23506053]
9. (a) Norcross RD, Paterson I. *Chem Rev.* 1995; 95:2041.(b) Shindo, M. Total synthesis of marine macrolides. In: Kiyota, H., editor. *Marine Natural Products.* Vol. 5. Springer; Berlin, Heidelberg: 2006. p. 179-254.
10. Kobayashi M, Higuchi K, Murakami N, Tajima H, Aoki S. *Tetrahedron Lett.* 1997; 38:2859.
11. Youssef DTA, Van Soest RWM, Fusetani N. *J Nat Prod.* 2003; 66:679, 861. [PubMed: 12762806]
12. Buchanan MS, Carroll AR, Addepalli R, Avery VM, Hooper JNA, Quinn RJ. *J Nat Prod.* 2007; 70:2040. [PubMed: 18027906]
13. Ibrahim SRM, Min CC, Teuscher F, Ebel R, Kakoschke C, Lin W, Wray V, Edrada-Ebel R, Proksch P. *Bioorg Med Chem.* 2010; 18:4947. [PubMed: 20599387]
14. (a) Pham C-D, Weber H, Hartmann R, Wray V, Lin W, Lai D, Proksch P. *Org Lett.* 2013; 15:2230. [PubMed: 23582084] (b) Pham C-D, Hartmann R, Müller WEG, de Voogd N, Lai D, Proksch P. *J Nat Prod.* 2013; 76:103. [PubMed: 23282083] (c) Niemann H, Lin W, Müller WEG, Kubbutat M, Lai D, Proksch P. *J Nat Prod.* 2013; 76:121. [PubMed: 23249297]
15. Horst K. *Angew Chem, Int Ed Engl.* 1982; 21:512.
16. (a) Sandler JS, Colin PL, Kelly M, Fenical W. *J Org Chem.* 2006; 71:7245. [PubMed: 16958517] (b) Matsumori N, Kaneno D, Murata M, Nakamura H, Tachibana K. *J Org Chem.* 1999; 64:866. [PubMed: 11674159]
17. Ohtani I, Kusumi T, Kashman Y, Kakisawa H. *J Am Chem Soc.* 1991; 113:4092.
18. Ashour M, Edrada R, Ebel R, Wray V, Watjen W, Padmakumar K, Müller WEG, Lin WH, Proksch P. *J Nat Prod.* 2006; 69:1547. [PubMed: 17125219]



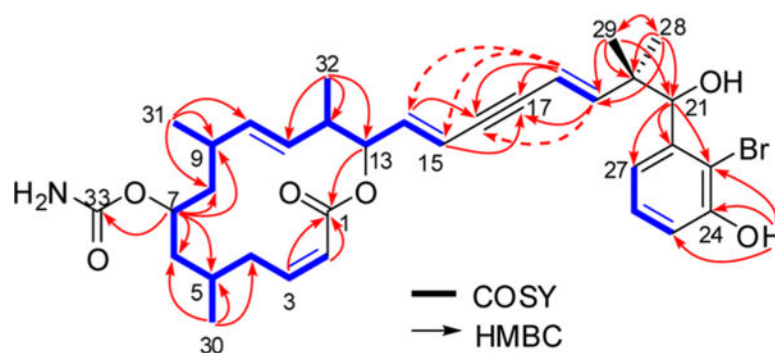


**Figure 1.**  
Key COSY and HMBC correlations of **1**.

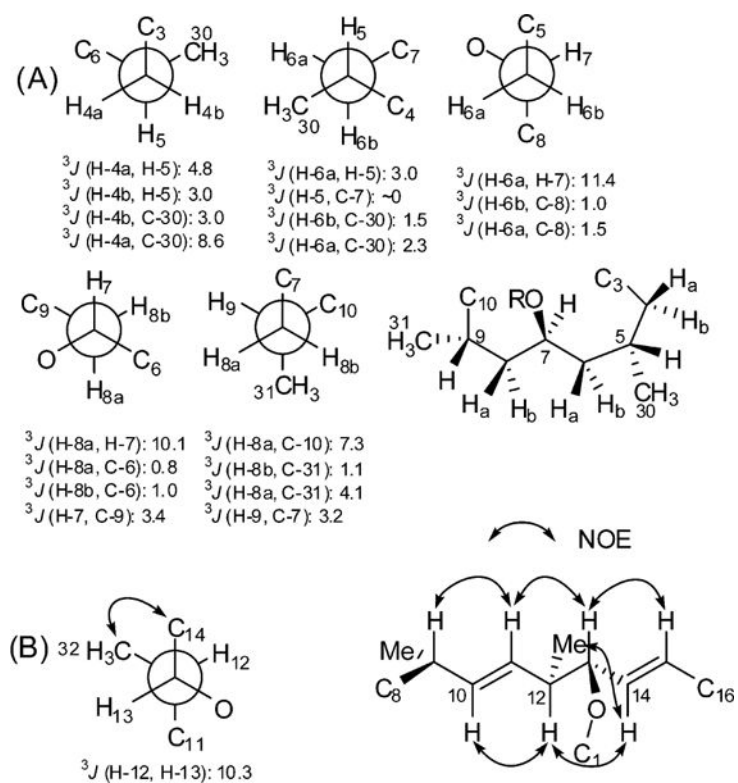


**Figure 2.** Conformational analyses for the macrocyclic region of **1**. (A) Rotamers determined for C4–C9 unit. (B) Rotamer determined for C12–C13 and key NOE correlations for C9–C13 backbone.